In vitro anti-tubulin effects of mebendazole and fenbendazole on J3T canine glioma cells

by

Serene Ruth Lai

A thesis submitted to the Graduate Faculty of
Auburn University
in partial fulfillment of the
requirements for the Degree of
Master of Science

Auburn, Alabama
December 10, 2016

Keywords: benzimidazole, chemotherapy,
mebendazole, fenbendazole, glioma, canine

Approved by

Jennifer (Jey) Koehler, Chair, Assistant Professor of Pathobiology
Jill Narak, Nonacademic member of the committee
Amanda Taylor, Assistant Professor of Clinical Sciences
Bruce Smith, Professor of Scott-Ritchey Research

Abstract

Benzimidazole anthelmintics have reported anti-neoplastic effects both *in vitro* and *in vivo*. The purpose of this study was to evaluate the *in vitro* chemosensitivity of canine glioma J3T cells to mebendazole and fenbendazole.

The mean IC_{50} (+/- SD) obtained from performing the MTT [3-(4,5-dimethylthiazol-2-yl)-2,5-diphenyltetrazolium bromide] assay after treating J3T cells for 72 hours with mebendazole and fenbendazole were 0.030 +/- 0.003 and 0.550 +/- 0.015 µM respectively. Tubulin polymerization assay showed a trend towards increased solubilized α-tubulin fractions with treatment, although no statistical significance was determined. Immunofluorescence studies showed disruption of tubulin after treatment.

Mebendazole and fenbendazole are cytotoxic in canine glioma J3T cells *in vitro* and may be good candidates for treatment of canine gliomas. Further *in vivo* studies evaluating pharmacokinetics of mebendazole and fenbendazole in the cerebrospinal fluid and subsequent antitumoral efficacy are indicated.

Acknowledgements

Table of Contents

List of Tables

List of Figures

List of Abbreviations

BZD	Benzimidazole
BBB	Blood brain barrier
CSF	Cerebrospinal fluid
KDR	Kinase insert domain receptor
DLL3	Delta-like 3 (Drosophila)
FBZ	Fenbendazole
GB	Glioblastoma
GBM	Glioblastoma multiforme
IC_{50}	Half maximal inhibitory concentration
MBZ	Mebendazole
MGMT	O6-methylguanine-DNA methyltransferase
MTT	MTT [3-(4,5-dimethylthiazol-2-yl)-2,5-diphenyltetrazolium bromide]
PDGFRA	Platelet derived growth factor receptor alpha
PI3K	Phosphatidylinositol-4,5-bisphosphate 3-kinase
PTEN	Phosphatase and tensin homolog
RB1	Retinoblastoma 1
VEGF	Vascular endothelial growth factor
WHO	World Health Organization

INTRODUCTION

Gliomas comprise primary brain tumors of glial or glial progenitor origin that have morphologic differentiation toward astrocyte (astrocytomas), oligodendrocyte (oligodendrogliomas), ependymal cell (ependymomas), or mixed glial cell (oligoastrocytoma) lineages. Glioblastoma (GB) is a grade IV glioma as classified by the World Health Organization (WHO) and is considered the most malignant and invasive subtype. This tumor is also commonly referred to in the literature and in public discourse as glioblastoma multiforme (GBM), despite the removal of the "multiforme" term by the WHO after 2000. The classification of astrocytomas according to the 2007 WHO criteria predominantly relies on recognition of cytological features and is subject to inter-observer variation. However, cytological characterization of gliomas based on the WHO classification scheme are not reliably associated with tumor progression and treatment response.[1]

Emerging new data regarding the molecular profiles of diffuse infiltrating gliomas in humans has enabled subtyping of gliomas. Subtyping and molecular profiling of tumors are important for a more accurate diagnosis of tumor cell type and for prognostication and therapeutic recommendations. For example, chromosomal abnormalities such as 1p/19q codeletion may aid in identifying oligodendrogliomas[1] and is significantly associated with chemosensitivity while loss of heterozygosity of 10q is associated with a poor outcome.[2, 3] *O6-methylguanine-DNA methyltransferase (MGMT)* promotor methylation of gliomas is associated with a positive response to chemotherapeutic treatment with temozolomide.[1] Other molecular biomarkers include mutations in *isocitrate dehydrogenase 1* and *2* (*IDH1* and *IDH2*), distinctive epigenetic CpG island methylation profile, and mutations in *telomerase reverse transcriptase (TERT)* promotor

region.[1, 4] A study that performed gene expression profiling of 76 high grade gliomas such as anaplastic astrocytoma (III) and GB showed clustering of these tumors into three distinct prognostic subclasses.[5] Namely, high grade gliomas expressing normal neuronal lineage markers were associated with longer survival while tumors expressing markers associated with proliferation or mesenchymal tissues were associated with a poorer prognosis regardless of tumor grade, even if they were classified as GB.[5] Indeed, when gliomas recur, they tend to shift towards a mesenchymal molecular signature, and with evidence of increased angiogenesis.[5] Glioma cell lines with proliferation and mesenchymal molecular signatures were associated with neurosphere formation,[5] which is a significant independent predictor of glioma tumor progression and clinical outcome.[6] The formation of neurospheres is a feature of neural stem and progenitor cells, in which cells form aggregates when cultured *in vitro* in serum-free media.[7] Low *phosphatase and tensin homolog* (*PTEN*) expression was associated with a poor outcome regardless of *delta-like 3 (Drosophila)* [*DLL3*] expression but coexpression of high levels of *PTEN* and *DLL3* correlated with a good prognosis.[5] Consequently, studies reevaluating previously diagnosed gliomas using newly reported biomarkers revealed that approximately 80% of tumors originally diagnosed as diffuse or anaplastic astrocytomas were misdiagnosed and were in fact GB,[4] which may explain why previous studies based on histological characterization alone have failed to provide completely accurate associations between tumor subtype and response to treatment.

Information regarding genomic subtyping of canine gliomas is sparse. Preliminary studies indicate similarity in aberrant genes involved with gliomagenesis in both human[8] and canine[9] patients are associated with 3 critical pathways, namely *TP53*, *retinoblastoma 1* (*RB1*), and *RTK/RAS/PI3K*. In a study documenting the incidence of tumor suppressor *TP53* mutation in 18 canine astrocytomas, 14 oligodendrogliomas, and 4 mixed gliomas, the frequency of *TP53* mutations in all gliomas combined were 5.3%.[10] This incidence of *TP53* mutations in canine gliomas is markedly lower than that reported in humans in comparison, where the frequency of *TP53* mutation is 60-80% in low grade (II) and high grade anaplastic (III) astrocytomas, 65% in

secondary GB that developed from a lower grade glioma, and 10% in *de novo* GB.[10] Despite a low incidence of *TP53* mutations in canine gliomas, altered TP53 protein levels were consistently detected in astrocytic tumors. In particular, TP53 is found to be elevated in 2/3 of astrocytomas when compared to oligodendrogliomas and normal brain samples, indicating that the TP53 pathway may be associated with tumorigenesis of gliomas in dogs.[11] Canine studies regarding vascular endothelial growth factor (VEGF) parallel findings in humans. While both astrocytomas and oligodendrogliomas express increased levels of *VEGF*, astrocytomas tend to express more *VEGF* than oligodendrogliomas.[12] In addition, high grade astrocytoma (IV) and oligodendroglioma (III) showed increased *VEGF* expression, while lower grade gliomas, astrocytoma (II) express lower levels of *VEGF*.[12, 13] Expression of *TERT* was also found to be significantly associated with histological grade of brain tumors, including gliomas.[14] Oligodendrogliomas were associated with loss of *RB1* and *TP73*, amplification of *platelet derived growth factor receptor alpha* (*PDFGRA*), *kinase insert domain receptor* (*KDR*), and *KIT*, and chromosomal losses syntenic to human 1p.[9] Further, canine GB are associated with loss of *INK4A/B* locus.[9] Information correlating therapeutic response and molecular profiling is not yet available in the dog.

In human patients in the United States, gliomas represent 25.2% of primary central nervous system (CNS) tumors, making them the second most common histologic type.[15] Of these, approximately half are GB.[15] In canine patients the percentage of gliomas is similar, with this histologic type representing approximately a third of all primary CNS tumors.[16, 17] However, GB as a percentage of gliomas in dogs in two retrospective necropsy studies was estimated at 1.2%[17] to 8%[16]. This is far less than the approximately 50% reported in humans, but may be reflective of some selection bias in the studied canine population. Brachycephalic dogs, including English and French bulldogs, Boston terriers, and Boxers, are predisposed to developing gliomas.[17] Canine GB have a similar appearance to human GB on imaging, grossly, and histologically, and have been reported in the cerebrum, thalamus, cerebellum, brainstem, and spinal cord.[18-20]

3

In humans, the standard of care for GB currently consists of surgical resection in combination with radiotherapy and the DNA-alkylating/methylating chemotherapy agent temozolomide. Seventy-three percent of human patients die within 2 years of diagnosis of GB despite treatment.[21] The standard therapeutic options for dogs currently consist of surgical cytoreduction and/or radiation therapy. However, because of financial constraints and/or personal choice, only a small percentage of the client population pursues full diagnostic workup and therapy for these patients. Many dogs do not reach their natural endpoint because owners elect humane euthanasia. These features, in addition to inherent differences in patient size and genetic variability, tumor biology, and diagnostic and clinical expertise make it difficult to accurately compare human and canine patient outcomes in response to therapy. Understandably due to these constraints, there is sparse information regarding treatment and corresponding survival times in dogs. A retrospective survival study of dogs diagnosed with intra-axial tumors suspected to be gliomas reported a median survival of 120 days with radiation therapy.[22] This median survival time is similar to dogs with intracranial neoplasms that received only palliative care reported in another study, in which dogs with supratentorial neoplasms had a median survival of 178 days and those with infratentorial neoplasms had a significantly shorter median survival of 28 days.[23] A recent case study reported a 2.5-year survival in a dog with anaplastic oligodendroglioma treated with radiation therapy and CCNU.[24]

Although there are many clinical trials available for human GB, few show clear survival benefit, thus emphasizing the need for further investigation into novel therapeutic options in both human and veterinary medicine. Benzimidazole (BZD) compounds have been used traditionally in human and veterinary medicine to treat parasitic infections, though investigation into their use as anti-neoplastic agents began as early as the 1950s.[25] The resurgence of the idea of using BZDs as antineoplastic therapy for glioblastoma arose serendipitously when SCID nude mice in well-established lymphoma[26] and brain tumor[27] xenograft models to study tumorigenesis received fenbendazole (FBZ) treatment for pinworms. Treated animals were reported to experience

disruption in tumor engraftment, which sparked renewed interest into investigating the cytotoxic and anti-proliferative mechanisms of BZDs. Since then, multiple human studies have shown anti-tumor effects of BZDs in neoplasms as diverse as melanoma,[28] non-small cell lung cancer,[29] ovarian cancer,[30] hepatocellular carcinoma,[31] and leukemia.[32]

The half-maximal inhibitory concentration (IC_{50}) is defined as the concentration of a substance in which 50% of cell population dies. A study testing the efficacy of BZDs on a variety of melanoma cell lines showed the most striking growth-inhibitory effects of mebendazole (MBZ), as compared to other BZDs: albendazole, FBZ, and oxybendazole (table 1).[28] Twenty-four hours after treatment with 1 μM MBZ, 25-31% of melanoma cells underwent apoptosis compared with 5% of non-neoplastic immortalized melanocytes, suggesting that mebendazole results in a differential cytotoxicity with preferential induction of apoptosis in melanoma cells while exerting minimal effects in their non-neoplastic counterparts.[28] In 2002, antitumor and antiangiogenic effects of MBZ were demonstrated in *in vivo* and *in vitro* studies of human non-small cell lung cancer, while the drug had little effect on control normal fibroblast cells.[29, 33] Therefore, there is accumulating evidence that BZDs have efficacy against a variety of tumors, with minimal adverse effects on normal cells.

Table 1: IC_{50} of benzimidazoles that display growth inhibition in melanoma (SK-Mel-19 and M-14) cell lines as compared with melanocytes (Melan-a).[28]

	Melan-a μM	SK-Mel-19 μM	M-14 μM
Mebendazole	1.9	0.3	0.32
Albendazole	3.8	0.7	1.2
Fenbendazole	3.4	1.2	1.4
Oxybendazole	3.5	0.8	1.1

Treatment for intracranial tumors including GB are limited by the inability of many drugs to cross the blood-brain barrier (BBB), making it challenging to achieve adequate concentration of drugs within the central nervous system. Due to their small size and lipophilic nature, BZDs

have the ability to penetrate the BBB.[27, 34] Indeed, FBZ, a widely-used veterinary BZD, has been used to successfully treat intracranial parasites in dogs,[35] emphasizing that FBZ can cross the BBB and is able to reach levels within the CNS adequate for its anti-parasitic action. Furthermore, a study in 2011 using MBZ showed survival benefit in preclinical mouse models of GB,[27] demonstrating the possible ability of the BZD compound to exert antineoplastic effects intracranially.

The main mode of action of BZDs is the disruption of tubulin and inhibition of mitotic spindle formation, thereby resulting in mitotic arrest and further leading to apoptosis.[29, 31, 33, 36] Microtubules consist of repeating α and β-tubulin heterodimers, are present in all eukaryotes, and are involved in an extensive variety of cellular functions, including maintenance of cellular shape, organelle/protein transport, cell motility, and cell division.[37] The inherent property necessary for their functionality is "dynamic instability", which means that they can switch stochastically between shrinking and growing phases.[37] Microtubules such as tubulin are well recognized as effective targets for anticancer therapy. Microtubule-targeted chemotherapeutics such as paclitaxel, colchicine, and vinca alkaloids exert their inhibitory effect on cancer cell proliferation primarily by increasing microtubule stability or by depolymerization, resulting in disruption of the mitotic spindle. This causes cell cycle arrest at the G_2-M phase (mitotic checkpoint) and induces apoptosis.[31]

Tubulin binding studies comparing the effect of eleven BZDs on tubulin from purified bovine brain showed differences in structural specificity and binding affinities amongst the compounds. Although the conserved nature of the tubulin protein has been shown based on amino acid sequence analysis of NH_2-terminal regions of α and β tubulins[38] and by tubulin copolymerization experiments,[39, 40] differential binding affinities between nematode tubulin and mammalian tubulin may explain how for example, mebendazole can interfere with the microtubule system of *Ascaris suum*, while sparing host microtubules.[41] Tubulin binding studies

also indicate BZDs bind at a site similar to colchicine[42] while paclitaxel and vinblastine bind at the taxol and vinblastine sites respectively.[43] Not surprisingly, there is evidence that combining microtubule-targeting drugs with different modes of action or different binding sites results in a synergistic effect.[44]

Recent literature has elucidated that BZDs can induce cell death via multiple pathways, which is not surprising given the reliance of cells on microtubules for a multitude of cell cycle processes. Cell cycle regulators such as TP53 and TP21 have also been shown to be elevated in BZD treated cells[29] and it is suspected that TP53 may mediate BZD-induced apoptosis.[36] TP53 relies on dynein-dependent transport along microtubules to the nucleus where its translocation allows it to execute its effects on transcription and cell-cycle modulation,[45] including upregulation of *p21*.[29, 33] Paradoxically, rapid and severe disruption of microtubules results in failure of TP53 trafficking to the nucleus and disruption of TP53-mediated events.[45] Furthermore, depletion of TP53 signaling has been shown to result in decreased chemosensitivity of a variety of tumor cells to flubendazole.[36] As previously mentioned, the incidence of *TP53* mutation in canine gliomas is reportedly lower than that of human gliomas.[10] Thus, canine gliomas may experience higher chemosensitivity than human gliomas, making BZDs a useful antineoplastic treatment.

Although TP53 signaling is one of the main pathways in which BZDs cause tumor death, there is also evidence that BZDs can induce cell death via TP53-independent pathways.[29, 33, 46] Specifically, MBZ has been shown to have growth-inhibitory effects on *p53*-null and *p53*-mutant cell lines although at a higher doses than *p53*-wild type cells, indicating a role for TP53-independent pathways for apoptosis.[33] After treatment of multiple human cancer cell lines with MBZ, there was a dose-dependent increase in cytochrome *c* protein and evidence of caspase activation.[33] In addition, treatment of the H460 human non-small cell carcinoma cell line with MBZ activated caspases 3, 8, and 9, further suggesting that MBZ can induce cell death involving a mitochondrial and caspase-dependent cascade.[29] BZDs also have antiangiogenic effects, inhibiting neovascularization of tumor cells *in vitro* and *in vivo,* with seemingly no effect on

7

normal endothelial cell growth.[33, 36] These collective findings highlight the multi-faceted nature of the effects of BZDs on tumor cells.

BZDs as a class of drugs have limited solubility in water and organic solvents and due to their lipophilic properties are capable of crossing the blood-brain barrier.[34] When administered orally, the absorption of albendazole has been reported to be 5-10% in humans.[47] Fatty meals are usually included to increase absorption in humans and rodents.[34, 47] In dogs, oral administration of FBZ at the anti-parasitic dose of 50 mg/kg/day reached a maximum plasma concentration (C_{max}) level of 0.16 ± 0.08 µg/ml (0.55 ± 0.27 µM).[48] Although safety studies of MBZ treatment have been performed on dogs,[49] there is no current data on C_{max} achieved in MBZ-treated dogs. In FDA-required safety studies of MBZ and FBZ performed in dogs, long-term oral administration of MBZ to purebred Irish Setters and Toy Poodles at 110 mg/kg/day (5 times the anthelmintic therapeutic dose of 22 mg/kg/day) and mixed-breed dogs at 11 to 110 times this same therapeutic dose for 2 months showed no adverse effects on liver function.[49] Furthermore, administration of MBZ at 330 mg/kg/day to dogs with experimentally-induced altered liver function in the same study did not result in hepatotoxicity.[49] In a series of unpublished reports submitted to the WHO, FBZ did not cause treatment-related effects in dogs administered oral dosages ranging from 20 to 125 mg/kg/day in a 90-day study[50] or 1 to 10 mg/kg/day in a 14-week study.[51] At higher doses, or in longer-term studies, mild FBZ treatment-related effects were observed.[52] Specifically, in dogs administered 80 and 250 mg/kg/day for 30 consecutive days there was lymphoid follicle proliferation and nodules in the gastric mucosa and low-grade diffuse centrilobular fatty degeneration in the liver .[52, 53] In this same study, three dogs given 125 mg/kg/day dose for 6 months had histologically evident mild, focal cerebral encephalomalacia, satellitosis, and neuronophagia (two dogs), or mild perivascular inflammation and gliosis (one dog), although it is worth noting that the dogs remained clinically asymptomatic.[52] Moreover, in humans, long-term treatment with MBZ for alveolar echinococcosis with dosages as high as 200 mg/kg/day for up to 48 weeks was well tolerated.[54] Cerebrospinal fluid (CSF) analysis from a patient in that study

8

receiving 200 mg/kg/day of MBZ attained a concentration of 8.6 ng/ml (0.0291 µM), although it was clear in that report that plasma and likely CSF levels may be highly variable depending on dose, dosing interval, and gastrointestinal absorption rate.[54]

These studies indicate the possibility of using MBZ and FBZ at higher doses and for longer durations than those required for antiparasitic treatment, with an acceptably low potential for significant treatment-related morbidity. To our knowledge, there are no published studies examining the use of BZDs in canine glioma. In this study, we evaluated the *in vitro* effects of MBZ and FBZ on cell viability and tubulin disruption in the J3T canine anaplastic astrocytoma cell line.

MATERIALS AND METHODS

Cell line

J3T canine anaplastic astrocytoma cell line (a generous gift from Dr. Michael Berens) was used for the experiments.[55-57] The J3T cell line was derived from *in vitro* clonal expansion (DL3580 c2) of a spontaneously occurring anaplastic glioma obtained from the thalamus of a 10-year old Boston Terrier.[55] The cell line was maintained on monolayer culture for a year and verified to have a stable karyoptype and same chromosomal markers as the parent cell line.[55] Although initially identified as a anaplastic (III) astrocytoma, subcutaneous and intracranial orthotopic xenograft implantation of DL3580 c2 into athymic mice revealed histologic characteristics that are reminiscent of GB.[55] Subcutaneous allogenic implantation of the J3T cell line into fetal Beagle pups on gestational day 37 also developed tumors with histological features of GB. However, subcutaneous and intracranial xenograft studies in severe combined immunodeficiency (SCID) mice produced anaplastic astrocytomas without evidence of invasiveness and necrosis as demonstrated that in the previous Beagle study. The J3T cell line has wild type *p53* expression[56] and has been previously verified to in our lab by species-specific PCR to be of dog origin and mycoplasma-free, and are nestin and glial fibrillary acidic protein (GFAP) immunopositive, confirming their glial origin.

Cell culture

J3T cells were cultured in standard polystyrene tissue culture flasks and plates in Dulbecco's Modified Eagle Medium (DMEM) containing 4.5 g/L glucose, 4 mM L-glutamate, and sodium

pyruvate (HyClone Laboratories, GE Healthcare Life sciences, South Logan, UT, USA) supplemented with 10% heat-inactivated fetal bovine serum (Seradigm, Radnor, PA, USA), 100U/ml penicillin, 100 μg/ml streptomycin, and 2.5 μg/ml amphotericin B (Corning Life Sciences, Tewksbury, MA, USA). Cells were incubated in 100% humidity at 37ºC, 20% O_2 and 5% CO_2.

Drug treatment and the MTT cell viability assay

J3T cells were seeded at 6,000 cells/well in 96-well plates, allowed to attach overnight, and then exposed to a range of drug concentrations for 72 h. The final concentrations evaluated were two-fold dilutions ranging from 3.0 to 0.006 μM for FBZ and 1.5 to 0.006 μM for MBZ. Media-only and no-treatment wells were included in all assays. All treatments were performed in quadruplicates. After 72 h of exposure to drugs, cell viability was assessed using the MTT assay (Biotium, Hayward, CA, USA) according to the manufacturer's protocols, and the colorimetric reaction was read using a microplate photospectrometer (Infinite M200, Tecan, Mannedorf, Switzerland).

Half-maximal inhibitory concentration (IC_{50})

Raw OD values from the microplate photospectrometer readings were analyzed using Graphpad Prism 6.07 software. IC_{50} values were generated using a four-parameter variable-slope curve fit nonlinear regression analysis.

Tubulin polymerization assay

Tubulin was measured as described previously with some modifications.[58] J3T cells were seeded at 2×10^5 cells/well onto a 6-well culture plate and incubated until 70-80% confluency. Cells were treated for 5-7 h with MBZ (0.03 and 0.12 μM) and FBZ (0.6 and 2.4 μM). Media-only and DMSO (5 μL with 2 ml of media per well) controls were used. Cells were washed with prewarmed HBSS buffer, removed using a cell scraper, and harvested in HBSS into microfuge

11

tubes. They were centrifuged at 15,000 g at 25-30ºC for 5 min, then the cell pellet was lysed with 200 µL prewarmed 37ºC NP40 cell lysis buffer (20 mM Tris HCl 1 mM $MgCl_2$ 2 mM EGTA, 0.5% NP40) and supplemented with protease inhibitors without EDTA (G-Biosciences, St. Louis, MO, USA). After subsequent centrifugation at 15,000 g at 25-30ºC for 30 min, the supernatant containing depolymerized tubulin was removed and incubated on ice. The pellet containing polymerized tubulin was resuspended in 200 µL NP40 lysis buffer supplemented with protease inhibitors and disrupted with sonication. All samples were snap-frozen in liquid nitrogen and stored at -80ºC until further analysis.

Antibody validation

Monoclonal mouse anti α-tubulin DM1A IgG (GeneTex, Irvine, CA, USA) was validated for use in this experiment via western blotting and immunofluorescence. J3T cell lysates constituted a positive control and probing of membranes with anti-tubulin antibody showed a single well-defined 50 kDa band. In the western blot experiments, negative controls consisted of omitting cell lysates. Negative control in the immunocytochemistry experiments consisted of omitting secondary antibody. In all negative controls, there was no evidence of nonspecific binding nor autofluorescense.

SDS-PAGE electrophoresis

Previously snap-frozen lysed cell pellets in NP40 lysis buffer described above were thawed on ice and diluted 1:10 with NP40 lysis buffer. Samples were mixed with 1x Laemmli buffer (Bio-Rad Laboratories, Hercules, CA, USA) supplemented with 5% ß-mercaptoethanol (Sigma-Aldrich, St. Louis, MO, USA) and incubated at 95ºC for 10 min. Proteins were separated by SDS-PAGE electrophoresis using a 12% Tris-glycine SDS polyacrylamide gel (Bio-Rad Laboratories) at 150 V for 45 min at room temperature. The proteins were transferred to polyvinylidene fluoride (PVDF) membrane (Bio-Rad Laboratories) at 35 V, 4ºC for 8 h.

Western Blot

The membrane was washed with Tris buffered saline with Tween 20 (TBST) [G-Biosciences] and blocked with LI-COR/PBS buffer (LI-COR Biosciences, Lincoln, NE, USA) for 1 h at room temperature and then incubated with monoclonal mouse anti-α-tubulin DM1A IgG (GeneTex) in a 1:1000 dilution with LI-COR/PBS buffer for 1 h at room temperature with shaking. The membrane was washed with TBST and incubated with Near-IR-CF770 dye labelled goat anti-mouse IgG (Biotium) in a 1:2000 dilution for 1 h and then washed with TBST. Bands were visualized using infrared imaging and software (LI-COR Odyssey with Image Studio Version 2.0).

Immunofluorescence

J3T cells were seeded at 10,000 cells per well into 8-well chamber slides (Nunc, Naperville, IL, USA) and allowed to adhere overnight, then exposed to 2.4 µM FBZ, 0.12 µM MBZ, or media only for 2 h. Cells were washed and fixed with prewarmed 4% paraformaldehyde for 10 min at room temperature and permeabilized with 0.5 % Triton X-100 (Biorad Laboratories) for 10 min at 4ºC. Cells were blocked with 1% bovine serum albumin (Amresco, Solon, OH, USA) for 30 min at room temperature and then incubated at room temperature for 1 h with primary monoclonal mouse anti-α-tubulin IgG (GeneTex) or monoclonal mouse anti-IgG (GeneTex) at 1:2000 followed by incubation with secondary polyclonal goat anti-mouse Alexa Fluor® 488 antibody labelled IgG (ThermoFisher Scientific, Waltham, MA, USA) at 1:500 for 1 h with shaking in a humidified chamber. Slides were mounted using DAPI-containing medium (Vector laboratories, Burlingame, CA, USA) for nuclei counterstaining, then examined with a Nikon A1 confocal microscope.

Statistical analysis

A Student's paired t-test was used to evaluate if the percentages of solubilized tubulin were

statistically significant for treated versus untreated J3T cells in the tubulin polymerization assay.

RESULTS

The use of the MTT assay as a means to measure viable cell numbers was validated in each cell line by creating a standard curve comparing the results of the MTT with absolute cell numbers as measured by manual counting using the hemocytometer and trypan blue method. MTT data and cell counts were determined to have a linear relationship (data not shown) and this validated the use of the MTT assay for evaluating cell viability in our experiments. To obtain the IC_{50}, J3T cells were treated with serial two-fold dilutions of MBZ (range of 1.5 to 0.006 µM) and FBZ (range of 3.0 to 0.006 µM) for 72 h. Wells containing cells without treatment and media-only wells were included as positive and negative controls respectively. Cell viability was determined by using the OD values obtained in wells after treatment and expressing them as a percentage of the OD values in wells containing cells without treatment. IC_{50} values were then generated using a four-parameter variable-slope curve fit nonlinear regression analysis. The mean IC_{50} (+/- SD) in J3T cells was 0.030 +/- 0.003 µM with MBZ treatment and 0.550 +/- 0.015 µM with FBZ treatment (Figure 1).

A tubulin polymerization assay was performed to demonstrate disruption of tubulin by comparing fractions of polymerized and solubilized tubulin after treating J3T cells with MBZ and FBZ at concentrations of 0.12 µM and 2.4 µM respectively. Because this is a dynamic assay, it was expected that the percentage of tubulin in the polymerized versus the solubilized fraction would vary widely among experiments.[58] Thus each solubilized fraction was expressed as a percentage of the total amount of α-tubulin in both the solubilized and polymerized fractions of the same sample within an experiment. Samples processed from untreated J3T cells contained a small of solubilized α-tubulin as compared to the polymerized fraction (Figure 2A). Treatment of

J3T cells with MBZ and FBZ resulted in an increased percentage of solubilized α-tubulin (Figure 2B). However, although this trend was consistent across experiments, a paired T-test did not show any statistical difference. The corresponding P values when comparing control to MBZ treatment was 0.25 and that of control and FBZ treatment was 0.07.

To further demonstrate disruption of tubulin on the cytoskeletal structure of glioma cells, immunofluorescence was performed to visualize the effects of treatment on α-tubulin *in situ*. When cells were treated with 0.12 μM MBZ and 2.4 μM FBZ for two hours, the normal filamentous and lacy appearance of tubulin was altered, with clumping of tubulin to the periphery of the cell and nuclear clumping (Figure 3).

DISCUSSION

Results from this study show high *in vitro* sensitivity of the J3T canine anaplastic

astrocytoma cell line to FBZ and MBZ. The concentrations required to reach IC_{50} for MBZ were

lower than that of FBZ. This is consistent with the limited studies in the human literature and may

indicate a difference in either drug availability, entry of drug into the cell, mode of action on

tubulin, or other cellular processes. Of most interest is that very low concentrations of both drugs

are required in our model to cause tumor cell death. In dogs, plasma concentration attained after

oral administration of 50 mg/kg/day of FBZ was 0.55 ± 0.27 µM [48]. To achieve higher

concentrations within the CNS, safety studies indicate that higher doses of FBZ can be

administered with minimal adverse effects.[50, 52] In addition, improving gastrointestinal absorption

of BZDs can increase plasma concentration and thus brain and CSF concentrations. A study in

mice involving administering MBZ polymorphs orally at 50 mg/kg achieved brain concentrations

equivalent to 7.1 µM.[34] Taken together, the IC_{50} concentrations of MBZ and FBZ obtained in this

study are likely achievable in both blood and CSF, although further studies into CNS

pharmacodynamics and distribution in the dog are needed.

The limitation for this project is that although there was a trend toward higher

percentages of solubilized tubulin with BZD treatment within each tubulin polymerization

experiment, the results were not statistically different across experiments performed on different

days. This was likely attributable to the inability to standardize the working temperature while

performing the experiments, in addition to the dynamic quality of tubulin. Cooler temperatures

have been shown to result in depolymerization of tubulin.[58] A temperature-controlled centrifuge

would be required to centrifuge the samples at the optimal temperature 37°C and that was not

available within the temporal and location constraints of the project. In addition, since samples cannot be processed concurrently, the time lapse between processing the first and last sample may also subject samples to temperature sampling variation. Difficulty getting the pellet containing polymerized fraction after centrifugation into suspension may also add to the inaccuracy of quantifying the amount of tubulin. Moreover, Western blotting is a semi-quantitative method of evaluating protein levels. Taken together, the tubulin polymerization assay can be utilized to trend changes in the amount of tubulin in each fraction (solubilized and polymerized), but should not be viewed as a means of quantifying the change. In order to demonstrate disruption of α-tubulin with MBZ and FBZ treatment in a more physiologically relevant way, cytoskeletal changes were visualized using immunofluoresence after BZD treatment. The immunofluorescence studies clearly verified disruption of α-tubulin due to treatment with MBZ and FBZ. Taken together, these experiments provide evidence for the disruption of tubulin as a result of BZD treatment.

In humans, temozolomide along with surgical resection and radiation therapy has become the standard of care for GB treatment based on a randomized, prospective study in 2005 of 573 newly-diagnosed human GB patients who underwent radiation therapy or radiation therapy plus temozolomide treatment, after surgical cytoreduction.[21] The study showed that the median survival was 14.6 months with radiation therapy plus temozolomide compared to 12.1 months with radiation therapy alone. The two-year survival rate was reported to be 26.5% with radiation therapy plus temozolomide and 10.3 percent with radiation therapy alone.[21] Based on these findings, temozolomide along with surgical resection and radiation therapy became the standard of care for GB, with recent studies adding evidence to a survival benefit adding temozolomide to standard radiation therapy.[59]

Unfortunately, not all patients will benefit equally from temozolomide treatment, a phenomenon primarily related to the various mechanisms of resistance inherent in individual

tumors. The most common mechanism for GB to develop resistance to alkylating agents such as temozolomide is via the enzyme O^6-alkylguanine-DNA alkytransferase, which is encoded by the *MGMT* gene. Methylation of the *MGMT* promoter region silences expression, allowing greater sensitivity of tumors to temolozomide.[60] Of 206 human GB assessed in one study, only 45% had *MGMT* promoter methylation; these patients achieved a median survival of 21.7 months with temozolomide and radiation therapy, as compared to 15.3 months with patients receiving only radiation therapy in the same group. In contrast, patients without *MGMT* promotor methylation receiving temozolomide and radiation therapy achieved a median survival time of 12.7 months, compared to 11.8 months for the same group of patients that received only radiation therapy. This shows that temozolomide only marginally increases survival time in GB patients without *MGMT* promotor methylation, or approximately one-half of the GB patient population.[61] As of this writing, there is no current published work evaluating *MGMT* promoter methylation status of canine GB.

With regard to the sensitivity of canine gliomas to temozolomide, little work has been published. Investigations in our lab into the IC_{50} for temozolomide in these three canine cell lines suggest minimal sensitivity to the drug (data not published), a finding corroborated by the work of the Dickinson lab that showed an IC_{50} of over 1 mM for beige mouse-passaged J3T cells (J3TBg) cells.[11] In contrast, a recent study determined the IC_{50} for several human GB cell lines after 72 h and reported a range from 14.1 to 234.6 μM.[62] A study of eight human GB and one mouse GB cell lines showed IC50 ranging from 8.7 to 547 μM when treated with temozolomide, compared to IC_{50} between 0.11 and 0.31 μM with MBZ treatment.[27] This wide range of IC_{50} of GB cells treated with temozolomide likely reflects the presence of multiple drug resistance mechanisms. Pharmacokinetics studies in 35 human patients diagnosed with glioma and receiving oral temozolomide therapy reported plasma levels ranging from 0.1 to 13.99 μg/ml (0.52 – 72 μM) and 0.16 to 1.93 μg/ml (0.82 – 9.95 μM) in CSF,[63] which may not be adequate for

chemosensitivity against GB. However, there is evidence that temozolomide accumulates within the central nervous system and that it may be the cumulative dose, rather than systemic or cerebral exposure that determines efficacy and safety.[63] Taken together, although temozolomide is currently a mainstay therapy for GB in humans, a significant population of patients show resistance to temozolomide. In addition, it remains to be proven whether it has enough value in the treatment of canine patients to justify its significant financial cost.

In addition to the specific resistance mechanisms of some GB to temozolomide, a general mechanism of drug resistance in many tumor types is associated with expression of ATP-binding cassette (ABC) transporters, which function as efflux pumps.[64] In a study by Michaelis et al,[36] ABCB1 expression enhanced a neuroblastoma cell line resistance to ABCB1 substrate, vincristine, but did not result in resistance to the BZD flubendazole. Further, the ABCB1 inhibitor, verapamil, increased sensitivity of ABCB1-expressing neuroblastoma cells to vincristine but did not alter flubendazole sensitivity.[36] These results are highly suggestive that resistance to BZDs may not associate with ABC transporter expression, as with other antitumor drugs, meaning that BZDs may be a viable adjunctive chemotherapeutic even in the face of multidrug resistance. Interestingly, resistance to benzimidazoles in parasites such as in hookworms[65], *Haemonchus contortus*[66], and other helminths[67] is associated with small nucleotide polymorphisms (SNPs) of *β-tubulin* and it is postulated that the mutations affect the tertiary structure of microtubules, thus preventing benzimidazole binding.[67]

In conclusion, this study quantitatively and qualitatively demonstrates the *in vitro* anti-tubulin effects and cytotoxicity of MBZ and FBZ on the J3T canine anaplastic astrocytoma cell line. Low IC$_{50}$ concentrations and potentially short drug exposure times necessary to achieve tumor cell death are desirable characteristics that recommend further investigation into the use of BZDs as anti-neoplastic agents in dogs. Multiple *in vivo* and *in vitro* studies have shown efficacy of these drugs against a variety of neoplasms with sparing effects on normal cells.[27, 28, 30, 31, 33] In addition, unlike many microtubule inhibitors, both MBZ and FBZ have high safety margins with

low morbidity, even when used at higher doses and longer treatment durations than those typically recommended for anthelmintic purposes. These features, combined with the fact that these drugs are relatively inexpensive, FDA-approved, and widely available, make them ideal candidates for use in veterinary patients.

FUTURE DIRECTION

The future direction of this project is to determine is to perform *in vivo* pharmacokinetic studies in order to determine drug concentrations achievable in plasma and CSF based on oral administration of mebendazole and fenbendazole and to evaluate whether these preliminary *in vitro* studies will be clinically applicable.

Three polymorphs of mebendazole (A, B, and C) have been documented via IR spectroscopy, each demonstrating different levels of penetration into the brain, side effects, and efficacy against glioma in a GL261 mouse model.[34] In this model, polymorphs B and C had increased ability to cross the BBB, were able to achieve a higher concentration in the brain far exceeding the IC_{50} of GL261 glioma cells, and were able to increase survival time. In contrast, treatment with polymorph A did not show any survival benefit, likely due to markedly low levels of drug in the plasma and brain.[34] Interestingly, polymorph B was associated with signfiant toxicity and resulted in weight loss and even fatality, although neither a necropsy or clinical evaluation was available to explain the adverse side effects.[34] This study provides strong evidence that *in vivo* studies of polymorphs of MBZ and FBZ may be essential to evaluate if there are species difference in pharmacokinetics, BBB penetration, efficacy, and toxicity.

Since the current recommendation for veterinary glioma patients includes cytoreduction surgery in conjunction with radiation therapy, it would be interesting to evaluate if adjunctive BZD treatment improves radiosensitivity of gliomas and extends survival times. Gliomas obtained during surgical procedures or biopsies should also be submitted for genetic testing to evaluate molecular signatures that may correlate chemosensitivity, radiation sensitivity, response to treatment, and survival outcome. In addition, since temozolomide is currently the

recommended chemotherapeutic agent for treatment in human patients with high grade gliomas, a similar study to evaluate adjunctive treatment of canine glioma patients with temozolomide alone and in conjunction with BZD would be interesting and relevant. Survival times can also be compared to patients that have not received surgery and radiation therapy but are treated with temozolomide, temozolomide and BZD, or palliatively with prednisone.

REFERENCES

1.   Vigneswaran K, Neill S and Hadjipanayis CG. Beyond the World Health Organization grading of infiltrating gliomas: advances in the molecular genetics of glioma classification. *Annals of Translational Medicine*. 2015; **3**(7): 95.

2.   Ramirez C, Bowman C, Maurage CA, Dubois F, Blond S, Porchet N and Escande F. Loss of 1p, 19q, and 10q heterozygosity prospectively predicts prognosis of oligodendroglial tumors-- towards individualized tumor treatment? *Neuro-Oncology*. 2010; **12**(5): 490-9.

3.   Thiessen B, Maguire JA, McNeil K, Huntsman D, Martin MA and Horsman D. Loss of heterozygosity for loci on chromosome arms 1p and 10q in oligodendroglial tumors: relationship to outcome and chemosensitivity. *Journal of Neuro-Oncology*. 2003; **64**(3): 271-8.

4.   Reuss DE, Kratz A, Sahm F, Capper D, Schrimpf D, Koelsche C, Hovestadt V, Bewerunge-Hudler M, Jones DT, Schittenhelm J, Mittelbronn M, Rushing E, Simon M, Westphal M, Unterberg A, Platten M, Paulus W, Reifenberger G, Tonn JC, Aldape K, Pfister SM, Korshunov A, Weller M, Herold-Mende C, Wick W, Brandner S and von Deimling A. Adult IDH wild type astrocytomas biologically and clinically resolve into other tumor entities. *Acta Neuropathologica*. 2015; **130**(3): 407-17.

5.   Phillips HS, Kharbanda S, Chen R, Forrest WF, Soriano RH, Wu TD, Misra A, Nigro JM, Colman H, Soroceanu L, Williams PM, Modrusan Z, Feuerstein BG and Aldape K. Molecular subclasses of high-grade glioma predict prognosis, delineate a pattern of disease progression, and resemble stages in neurogenesis. *Cancer Cell*. 2006; **9**(3): 157-73.

6.   Laks DR, Masterman-Smith M, Visnyei K, Angenieux B, Orozco NM, Foran I, Yong WH, Vinters HV, Liau LM, Lazareff JA, Mischel PS, Cloughesy TF, Horvath S and Kornblum

HI. Neurosphere formation is an independent predictor of clinical outcome in malignant glioma. *Stem Cells*. 2009; **27**(4): 980-7.

7.   Azari H, Louis SA, Sharififar S, Vedam-Mai V and Reynolds BA. Neural-colony forming cell assay: an assay to discriminate bona fide neural stem cells from neural progenitor cells. *J Vis Exp*. 2011; (49).

8.   Cancer Genome Atlas Research N. Comprehensive genomic characterization defines human glioblastoma genes and core pathways. *Nature*. 2008; **455**(7216): 1061-8.

9.   Dickinson PJ, York D, Higgins RJ, LeCouteur RA, Joshi N and Bannasch D. Chromosomal Aberrations in Canine Gliomas Define Candidate Genes and Common Pathways in Dogs and Humans. *Journal of Neuropathology and Experimental Neurology*. 2016; **75**(7): 700-10.

10.   York D, Higgins RJ, LeCouteur RA, Wolfe AN, Grahn R, Olby N, Campbell M and Dickinson PJ. TP53 mutations in canine brain tumors. *Veterinary Pathology*. 2012; **49**(5): 796-801.

11.   Boudreau CE, York D, Higgins RJ, LeCouteur RA and Dickinson PJ. Molecular signalling pathways in canine gliomas. *Veterinary and Comparative Oncology*. 2015.

12.   Rossmeisl JH, Duncan RB, Huckle WR and Troy GC. Expression of vascular endothelial growth factor in tumors and plasma from dogs with primary intracranial neoplasms. *American Journal of Veterinary Research*. 2007; **68**(11): 1239-45.

13.   Dickinson PJ, Sturges BK, Higgins RJ, Roberts BN, Leutenegger CM, Bollen AW and LeCouteur RA. Vascular endothelial growth factor mRNA expression and peritumoral edema in canine primary central nervous system tumors. *Veterinary Pathology*. 2008; **45**(2): 131-9.

14.   Long S, Argyle DJ, Nixon C, Nicholson I, Botteron C, Olby N, Platt S, Smith K, Rutteman GR, Grinwis GC and Nasir L. Telomerase reverse transcriptase (TERT) expression and proliferation in canine brain tumours. *Neuropathology and Applied Neurobiology*. 2006; **32**(6): 662-73.

15.   Ostrom QT, Gittleman H, Fulop J, Liu M, Blanda R, Kromer C, Wolinsky Y, Kruchko C and Barnholtz-Sloan JS. CBTRUS Statistical Report: Primary Brain and Central Nervous System Tumors Diagnosed in the United States in 2008-2012. *Neuro-Oncology*. 2015; **17 Suppl 4**: iv1-iv62.

16.   Snyder JM, Shofer FS, Van Winkle TJ and Massicotte C. Canine intracranial primary neoplasia: 173 cases (1986-2003). *Journal of Veterinary Internal Medicine*. 2006; **20**(3): 669-75.

17.   Song RB, Vite CH, Bradley CW and Cross JR. Postmortem evaluation of 435 cases of intracranial neoplasia in dogs and relationship of neoplasm with breed, age, and body weight. *Journal of Veterinary Internal Medicine*. 2013; **27**: 1143-52.

18.   Lipsitz D, Higgins RJ, Kortz GD, Dickinson PJ, Bollen AW, Naydan DK and LeCouteur RA. Glioblastoma multiforme: clinical findings, magnetic resonance imaging, and pathology in five dogs. *Veterinary Pathology*. 2003; **40**(6): 659-69.

19.   Rothlisberger A, Lehmbecker A, Beineke A, Mischke R, Dziallas P, Meyer-Lindenberg A and Tipold A. Suspected primary glioblastoma multiforme in the canine spinal cord. *Journal of Small Animal Practice*. 2012; **53**(10): 604-7.

20.   Lenz SD, Janovitz EB and Lockridge K. An anaplastic astrocytoma (glioblastoma) in the cerebellum of a dog. *Veterinary Pathology*. 1991; **28**(3): 250-2.

21.   Stupp R, Mason WP, van den Bent MJ, Weller M, Fisher B, Taphoorn MJ, Belanger K, Brandes AA, Marosi C, Bogdahn U, Curschmann J, Janzer RC, Ludwin SK, Gorlia T, Allgeier A, Lacombe D, Cairncross JG, Eisenhauer E, Mirimanoff RO, European Organisation for R, Treatment of Cancer Brain T, Radiotherapy G and National Cancer Institute of Canada Clinical Trials G. Radiotherapy plus concomitant and adjuvant temozolomide for glioblastoma. *New England Journal of Medicine*. 2005; **352**(10): 987-96.

22.   Brearley MJ, Jeffery ND, Phillips SM and Dennis R. Hypofractionated Radiation Therapy of Brain Masses in Dogs: A Retrospective Analysis of Survival of 83 Cases (1991–1996). *Journal of Veterinary Internal Medicine*. 1999; **13**: 408-12.

23.	Rossmeisl JH, Jr., Jones JC, Zimmerman KL and Robertson JL. Survival time following hospital discharge in dogs with palliatively treated primary brain tumors. *Journal of the American Veterinary Medical Association*. 2013; **242**(2): 193-8.

24.	Hasegawa D, Uchida K, Kuwabara T, Mizoguchi S, Yayoshi N and Fujita M. Long-term survival in a dog with anaplastic oligodendroglioma treated with radiation therapy and CCNU. *Journal of Veterinary Medical Science*. 2012; **74**(11): 1517-21.

25.	Rintelen K and Knobloch W. [Influence of benzimidazole derivatives on mouse ascites tumors. I]. *Acta Biologica et Medica Germanica*. 1958; **1**(1): 109-13.

26.	Gao P, Dang CV and Watson J. Unexpected antitumorigenic effect of fenbendazole when combined with supplementary vitamins. *Journal of the American Association for Laboratory Animal Sciences*. 2008; **47**(6): 37-40.

27.	Bai RY, Staedtke V, Aprhys CM, Gallia GL and Riggins GJ. Antiparasitic mebendazole shows survival benefit in 2 preclinical models of glioblastoma multiforme. *Neuro-Oncology*. 2011; **13**(9): 974-82.

28.	Doudican N, Rodriguez A, Osman I and Orlow SJ. Mebendazole induces apoptosis via Bcl-2 inactivation in chemoresistant melanoma cells. *Molecular Cancer Research*. 2008; **6**(8): 1308-15.

29.	Sasaki J-i, Ramesh R, Chada S, Gomyo Y, Roth JA and Mukhopadhyay T. The anthelmintic drug mebendazole induces mitotic arrest and apoptosis by depolymerizing tubulin in non-small cell lung cancer cells. *Molecular Cancer Therapeutics*. 2002; **1**: 1201–9.

30.	Chu SWL, Badar S, Morris DL and Pourgholami MH. Potent inhibition of tubulin polymerisation and proliferation of paclitaxel-resistant 1A9PTX22 human ovarian cancer cells by albendazole. *Anticancer Research*. 2009; **29**: 3791-6.

31.	Pourgholami MH, Woon L, Almajd R, Akhter J, Bowery P and Morris DL. In vitro and in vivo suppression of growth of hepatocellular carcinoma cells by albendazole. *Cancer Letters*. 2001; **165**: 43-9.

32.   Khalilzadeh A, Wangoo KT, Morris DL and Pourgholami MH. Epothilone-paclitaxel resistant leukemic cells CEM/dEpoB300 are sensitive to albendazole: Involvement of apoptotic pathways. *Biochemical Pharmacology*. 2007; **74**(3): 407-14.

33.   Mukhopadhyay T, Sasaki J-i, Ramesh R and Roth JA. Mebendazole Elicits a Potent Antitumor Effect on Human Cancer Cell Lines Both in Vitro and in Vivo. *Clinical Cancer Research*. 2002; **8**: 2963-9.

34.   Bai RY, Staedtke V, Wanjiku T, Rudek MA, Joshi A, Gallia GL and Riggins GJ. Brain Penetration and Efficacy of Different Mebendazole Polymorphs in a Mouse Brain Tumor Model. *Clinical Cancer Research*. 2015; **21**(15): 3462-70.

35.   Garosi LS, Platt SR, McConnell JF, Wrayt JD and Smith KC. Intracranial haemorrhage associated with Angiostrongylus vasorum infection in three dogs. *Journal of Small Animal Practice*. 2005; **46**(2): 93-9.

36.   Michaelis M, Agha B, Rothweiler F, Loschmann N, Voges Y, Mittelbronn M, Starzetz T, Harter PN, Abhari BA, Fulda S, Westermann F, Riecken K, Spek S, Langer K, Wiese M, Dirks WG, Zehner R, Cinatl J, Wass MN and Cinatl J, Jr. Identification of flubendazole as potential anti-neuroblastoma compound in a large cell line screen. *Scientific Reports*. 2015; **5**: 8202.

37.   Nogales E. Structural insights into microtubule function. *Annual Review of Biochemistry*. 2000; **69**: 277-302.

38.   Luduena RF and Woodward DO. Isolation and partial characterization of alpha and beta-tubulin from outer doublets of sea-urchin sperm and microtubules of chick-embryo brain. *Proceedings of the National Academy of Sciences of the United States of America*. 1973; **70**(12): 3594-8.

39.   Sheir-Neiss G, Nardi RV, Gealt MA and Morris NR. Tubulin-like protein from Aspergillus nidulans. *Biochemical and Biophysical Research Communications*. 1976; **69**(2): 285–90.

40.   Water RD and Kleinsmith LJ. Identification of α and β tubulin in yeast. *Biochemical and Biophysical Research Communications*. 1976; **70**(3): 704-8.

41.   Borgers M, DeNollin S, DeBrabander M and Thienpent D. Microtubules and microtubule inhibitors. North-Holland, Amsterdam, 1975.

42.   Friedman PA and Platzer EG. Interaction of anthelmintic benzimidazoles and benzimidazole derivatives with bovine brain tubulin. *Biochimica et Biophysica Acta*. 1978; **544**: 605-14.

43.   Jordan MA, Wendell K, Gardiner S, Derry WB, Copp H and Wilson L. Mitotic block induced in HeLa cells by low concentrations of paclitaxel (Taxol) results in abnormal mitotic exit and apoptotic cell death. *Cancer Research*. 1996; **56**(4): 816-25.

44.   Photiou A, Shah P, Leong LK, Moss J and Retsas S. In vitro synergy of paclitaxel (Taxol) and vinorelbine (Navelbine) against human melanoma cell lines. 1997; **33**(3): 463-70.

45.   Rovini A, Savry A, Braguer D and Carre M. Microtubule-targeted agents: when mitochondria become essential to chemotherapy. *Biochimica et Biophysica Acta*. 2011; **1807**(6): 679-88.

46.   Bai RY, Staedtke V, Rudin CM, Bunz F and Riggins GJ. Effective treatment of diverse medulloblastoma models with mebendazole and its impact on tumor angiogenesis. *Neuro-Oncology*. 2015; **17**(4): 545-54.

47.   Dayan AD. Albendazole, mebendazole and praziquantel. Review of non-clinical toxicity and pharmacokinetics. *Acta Tropica*. 2003; **86**(2-3): 141-59.

48.   Gokbulut C, Bilgili A, Hanedan B and McKellar QA. Comparative plasma disposition of fenbendazole, oxfendazole and albendazole in dogs. *Veterinary Parasitology*. 2007; **148**(3-4): 279-87.

49.   Van Cauteren H, Marsboom R, Vandenberghe J and Will JA. Safety studies evaluating the effect of mebendazole on liver function in dogs. *Journal of the American Veterinary Medical Association*. 1983; **183**(1): 93-8.

50.   Kramer and Schultes. A subchronic tolerance trial (90 days) with HOE 881 in dogs. In: *Hoechst-Roussel unpublished report submitted to WHO* edn., Frankfurt, am Main, Germany, HOECHST AG, 1974.

51.   Doerr B and Carmines E. Final report on 14-week oral toxicity study of fenbendazole in dogs. In: *Hoechst-Roussel unpublished report submitted to WHO,* edn., Frankfurt, am Main, Germany, Hoechst AG, 1983.

52.   Wazeter F and Goldenthal E. Six-month oral toxicity study in dogs In: *International Research and Development Corporation unpublished report submitted to WHO,* edn., Frankfurt am Main, Germany, Hoechst AG, 1977.

53.   Goldenthal E. Six-month oral toxicity study in dogs In: *International Research and Development Corporation unpublished report Submitted to WHO,* edn., Frankfurt am Main, Germany, Hoechst AG, 1978.

54.   Bryceson AD, Woestenborghs R, Michiels M and van den Bossche H. Bioavailability and tolerability of mebendazole in patients with inoperable hydatid disease. *Transactions of the Royal Society of Tropical Medicine and Hygiene*. 1982; **76**(4): 563-4.

55.   Berens ME, Bjotvedt G, Levesque DC, Rief MD, Shapiro JR and Coons SW. Tumorigenic, invasie, karyotypic, and immunocytochemical characteristics of clonal cell lines deried from a spontaneous canine anaplastic astrocytoma. *In Vitro Cellular and Developmental Biology*. 1993; **29A**: 310-8.

56.   Berens ME, Giese A, Shapiro JR and Coons SW. Allogeneic astrocytoma in immune competent dogs. *Neoplasia*. 1999; **1**(2): 107-12.

57.   Rainov NG, Koch S, Sena-Esteves M and Berens ME. Characterization of a canine glioma cell line as related to established experimental brain tumor models. *Journal of Neuropathology and Experimental Neurology*. 2000; **59**(7): 607-13.

58.   Poruchynsky MS, Kim J-H, Nogales E, Annable T, Loganzo F, Greenberger LM, Sackett DL and Fojo T. Tumor cells resistant to a microtubule-depolymerizing hemiasterlin analogue,

HTI-286, have mutations α- or β-tubulin and increased microtubule stability. *Biochemistry*. 2004; **43**: 13944-54.

59.   Strowd RE, Abuali I, Ye X, Lu Y and Grossman SA. The role of temozolomide in the management of patients with newly diagnosed anaplastic astrocytoma: a comparison of survival in the era prior to and following the availability of temozolomide. *Journal of Neuro-Oncology*. 2016; **127**(1): 165-71.

60.   Clarke J, Butowski N and Chang S. Recent advances in therapy for glioblastoma. *Archives of Neurology*. 2010; **67**(3): 279-83.

61.   Hegi ME, Diserens AC, Gorlia T, Hamou MF, de Tribolet N, Weller M, Kros JM, Hainfellner JA, Mason W, Mariani L, Bromberg JE, Hau P, Mirimanoff RO, Cairncross JG, Janzer RC and Stupp R. MGMT gene silencing and benefit from temozolomide in glioblastoma. *New England Journal of Medicine*. 2005; **352**(10): 997-1003.

62.   Perazzoli G, Prados J, Ortiz R, Caba O, Cabeza L, Berdasco M, Gonzalez B and Melguizo C. Temozolomide Resistance in Glioblastoma Cell Lines: Implication of MGMT, MMR, P-Glycoprotein and CD133 Expression. *PloS One*. 2015; **10**(10): e0140131.

63.   Ostermann S, Csajka C, Buclin T, Leyvraz S, Lejeune F, Decosterd LA and Stupp R. Plasma and cerebrospinal fluid population pharmacokinetics of temozolomide in malignant glioma patients. *Clinical Cancer Research*. 2004; **10**(11): 3728-36.

64.   Ughachukwu P and Unekwe P. Efflux pump-mediated resistance in chemotherapy. *Annals of Medical and Health Sciences Research*. 2012; **2**(2): 191-8.

65.   Furtado LF, Alves WP, Moreira TB, Costa Junior LM, Miranda RR and Rabelo EM. Standardization and application of the tetraprimer ARMS-PCR technique for screening of the E198A SNP in the beta-tubulin gene of hookworm populations in Brazil. *Veterinary Parasitology*. 2016; **224**: 65-7.

66.   Nagy G, Csivincsik A, Zsolnai A and Sugar L. Benzimidazole resistance in Haemonchus contortus recovered from farmed red deer. *Parasitology Research*. 2016.

67.   Furtado LF, de Paiva Bello AC and Rabelo EM. Benzimidazole resistance in helminths: From problem to diagnosis. *Acta Tropica*. 2016; **162**: 95-102.
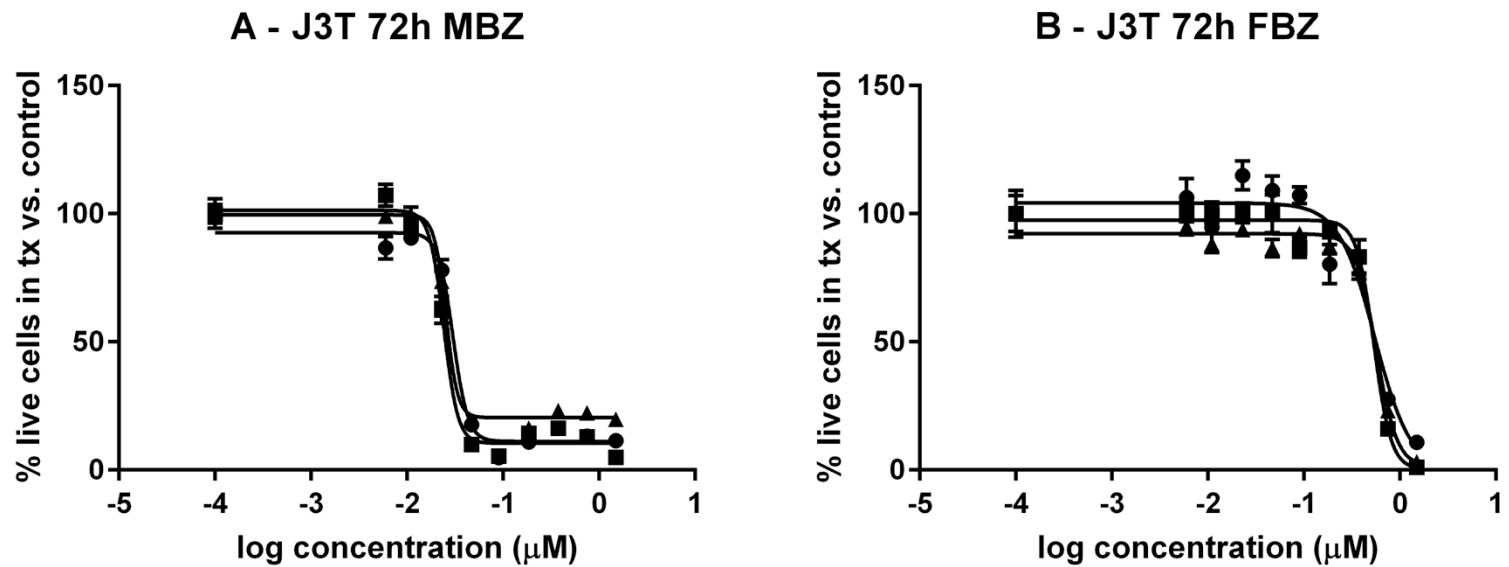
Figure 1: Each graph depicts the results of three separate experiments. J3T cells were treated with MBZ (A) and FBZ (B) for 72 h. The mean result of each data point in an individual experiment is depicted with a different shape (triangle, square, and circle). Standard deviation bars are included. Cell viability was measured using OD values obtained from the MTT assay and expressing them as a percentage of the OD values obtained in the wells of untreated cells. IC_{50} values were generated using a four-parameter variable-slope curve fit nonlinear regression analysis on data from MTT assays. The mean IC_{50} (+/- SD) obtained from treating J3T cells for 72 h with MBZ was 0.030 +/- 0.003 μM, while that of FBZ was 0.550 +/- 0.015 μM.
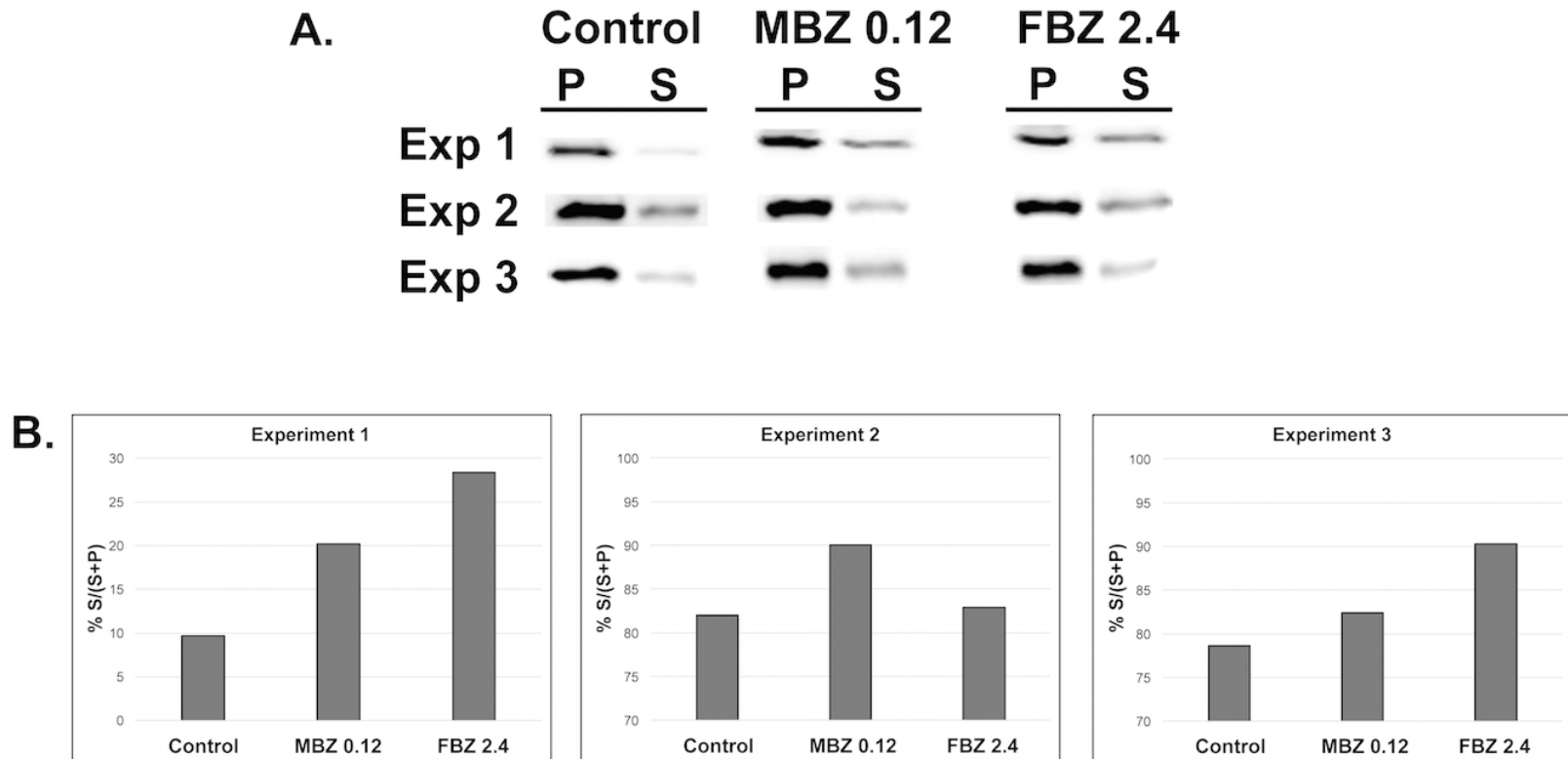
Figure 2: Tubulin polymerization experiments in J3T cells. A: Western blot showing polymerized (P) tubulin solubilized (S) tubulin from three independent experiments. Treatment with 0.12 μM MBZ and 2.4 μM FBZ resulted in increased solubilized tubulin fraction when compared to untreated cells. B: Bar graphs of percentage of solubilized vs. polymerized tubulin calculated as S/(S+P)*100% for corresponding experiments.
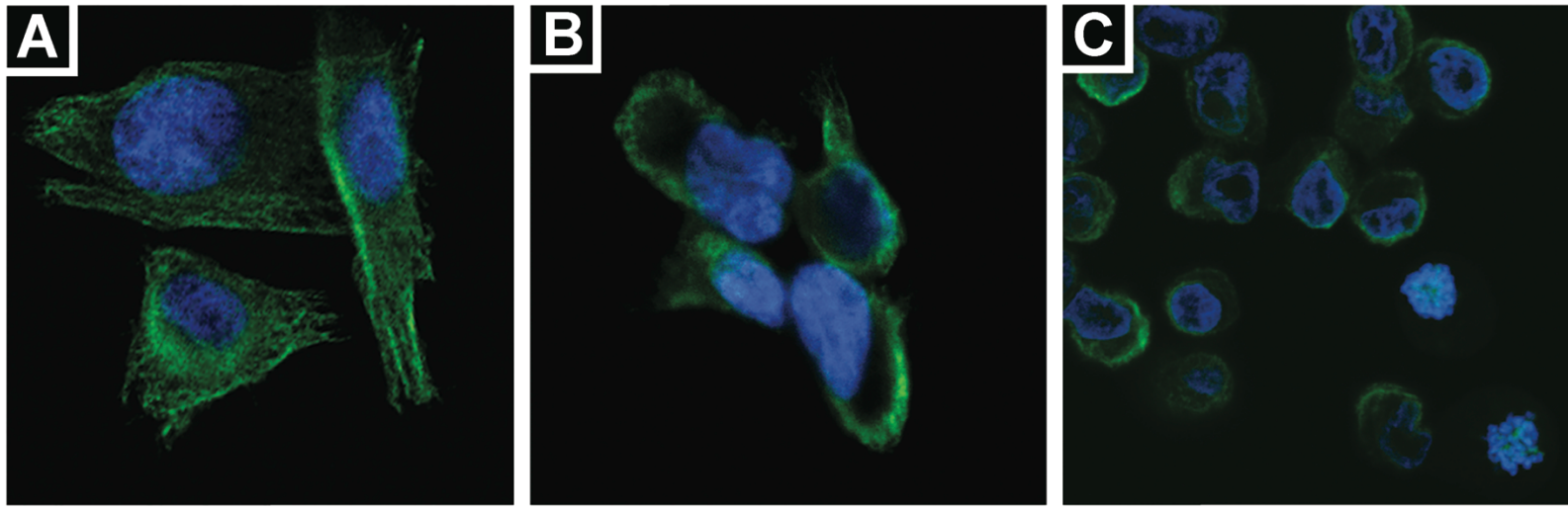
Figure 3: Immunofluorescence with anti-α-tubulin antibody in J3T cells. A: untreated, B: MBZ 0.12 μM, and C: FBZ 2.4 μM. The normally-distributed, lacy, filamentous tubulin network is seen in A (untreated) with normal cell morphology. In B and C (treated), the cells are contracted and tubulin is disrupted and clumped at the periphery of cells. In C, clumping of nuclear material is also noted. DAPI nuclear counterstain.